Springer Series in
MATERIALS SCIENCE 95

Springer Series in

MATERIALS SCIENCE

Editors: R. Hull R. M. Osgood, Jr. J. Parisi H. Warlimont

The Springer Series in Materials Science covers the complete spectrum of materials physics, including fundamental principles, physical properties, materials theory and design. Recognizing the increasing importance of materials science in future device technologies, the book titles in this series reflect the state-of-the-art in understanding and controlling the structure and properties of all important classes of materials.

78 **Macromolecular Nanostructured Materials**
Editors: N. Ueyama and A. Harada

79 **Magnetism and Structure in Functional Materials**
Editors: A. Planes, L. Mañosa, and A. Saxena

80 **Micro- and Macro-Properties of Solids**
Thermal, Mechanical and Dielectric Properties
By D.B. Sirdeshmukh, L. Sirdeshmukh, and K.G. Subhadra

81 **Metallopolymer Nanocomposites**
By A.D. Pomogailo and V.N. Kestelman

82 **Plastics for Corrosion Inhibition**
By V.A. Goldade, L.S. Pinchuk, A.V. Makarevich and V.N. Kestelman

83 **Spectroscopic Properties of Rare Earths in Optical Materials**
Editors: G. Liu and B. Jacquier

84 **Hartree–Fock–Slater Method for Materials Science**
The DV–X Alpha Method for Design and Characterization of Materials
Editors: H. Adachi, T. Mukoyama, and J. Kawai

85 **Lifetime Spectroscopy**
A Method of Defect Characterization in Silicon for Photovoltaic Applications
By S. Rein

86 **Wide-Gap Chalcopyrites**
Editors: S. Siebentritt and U. Rau

87 **Micro- and Nanostructured Glasses**
By D. Hülsenberg and A. Harnisch

88 **Introduction to Wave Scattering, Localization and Mesoscopic Phenomena**
By P. Sheng

89 **Magneto-Science**
Magnetic Field Effects on Materials: Fundamentals and Applications
Editors: M. Yamaguchi and Y. Tanimoto

90 **Internal Friction in Metallic Materials**
A Reference Book
By M.S. Blanter, I.S. Golovin, H. Neuhäuser, and H.-R. Sinning

91 **Time-dependent Mechanical Properties of Solid Bodies**
By W. Gräfe

92 **Solder Joint Technology**
Materials, Properties, and Reliability
By K.-N. Tu

93 **Materials for Tomorrow**
Theory, Experiments and Modelling
Editors: S. Gemming, M. Schreiber and J.-B. Suck

94 **Magnetic Nanostructures**
Editors: B. Aktas, L. Tagirov and F. Mikailov

95 **Nanocrystals**
Synthesis, Properties and Applications
By C.N.R. Rao, P.J. Thomas and G.U. Kulkarni

Volumes 30–77 are listed at the end of the book.

C.N.R. Rao P.J. Thomas G.U. Kulkarni

Nanocrystals: Synthesis, Properties and Applications

With 113 Figures, 6 in Color and 5 Tables

Springer

C.N.R. Rao, F.R.S.
P. J. Thomas
G.U. Kulkarni
Jawaharlal Nehru Center for Advanced Scientific Research
Jakkur P.O., Bangalore, 560 064 India
E-mail: cnrrao@jncasr.ac.in

ISSN 0933-033X

ISBN-10 3-540-68751-3 Springer Berlin Heidelberg New York

ISBN-13 978-3-540-68751-1 Springer Berlin Heidelberg New York

Library of Congress Control Number: 2006939006

Typesetting by SPi using a Springer LaTeX macro package
Cover concept: eStudio Calamar Steinen
Cover production: WMXdesign GmbH, Heidelberg

Printed on acid-free paper SPIN: 11304319 57/3100/SPi 5 4 3 2 1 0

Preface

Nanoscience has emerged to become one of the most exciting areas of research today and has attracted the imagination of a large body of students, scientists, and engineers. The various kinds of nanomaterials that one normally deals with are the zero-dimensional nanocrystals, one-dimensional nanowires and nanotubes, and two-dimensional nanofilms and nanowalls. Of these, one of the earliest research investigations pertains to nanocrystals. It is truly remarkable that Michael Faraday made nanocrystals of gold and other metals in solution way back in 1857. Nanocrystals occupy a special place amongst nanomaterials because they have enabled a proper study of size-dependent properties. There have been several reviews, books, and conference proceedings dealing with nanomaterials in the last few years. In this monograph, we have attempted to give a well-rounded presentation of various aspects of nanocrystals. We first discuss some of the fundamentals and then make a detailed presentation of the synthetic methods. We examine the process of assembly of nanocrystals as well as their properties. Core–shell nanoparticles are treated as a separate chapter, just as the applications of the nanocrystals. We believe that this monograph should be useful to practicing scientists, research workers, teachers, and students all over the world. It could also form the basis of a course on the subject.

Bangalore
January 2007

C.N.R. Rao
P.J. Thomas
G.U. Kulkarni

Contents

1

Basics of Nanocrystals

1.1 Introduction

Nanoparticles constitute a major class of nanomaterials. Nanoparticles are zero-dimensional, possessing nanometric dimensions in all the three dimensions. The diameters of nanoparticles can vary anywhere between one and a few hundreds of nanometers. Small nanoparticles with diameters of a few nanometers are comparable to molecules. Accordingly, the electronic and atomic structures of such small nanoparticles have unusual features, markedly different from those of the bulk materials. Large nanoparticles (>20–50 nm), on the other hand, would have properties similar to those of the bulk [1]. The change in a material property as a function of size is shown schematically in Fig. 1.1. At small sizes, the properties vary irregularly and are specific to each size. At larger sizes, dependence on size is smooth and scaling laws can be derived to describe the variation in this regime. The size-dependent properties of nanoparticles include electronic, optical, magnetic, and chemical characteristics. Nanoparticles can be amorphous or crystalline. Being small in size, crystalline nanoparticles can be of single domain. Nanoparticles of metals, chalcogenides, nitrides, and oxides are often single crystalline. Crystalline nanoparticles are referred to as nanocrystals.

Nanoparticles are not new and their history can be traced back to the Roman period. Colloidal metals were used to dye glass articles and fabrics and as a therapeutic aid in the treatment of arthritis. The Purple of Cassius, formed on reacting stannic acid with chloroauric acid, was a popular purple dye in the olden days. It is actually made up of tin oxide and Au nanocrystals [2]. The Romans were adept at impregnating glass with metal particles to achieve dramatic color effects. The Lycurgus cup, a glass cup of 4th century AD, appears red in transmitted light and green in reflected light. This effect, which can be seen in the cup preserved in the British museum in London, is due to Au and Ag nanocrystals present in the walls of the cup. Maya blue, a blue dye employed by the Mayas around 7th century AD has been shown recently to consist of metal and oxide nanocrystals in addition to indigo and silica [3].

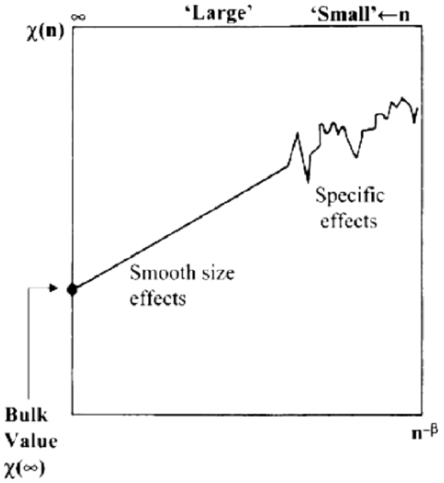

Fig. 1.1. The size dependence of a property $\chi(n)$ on the number of atoms (n) in a nanoparticle. The data are plotted against $n^{-\beta}$ where $\beta \geq 0$. Small nanoparticles reveal specific size effects, while larger particles are expected to exhibit a smooth size dependence, converging to the bulk value (reproduced with permission from [1])

Clearly, the ability to synthesize nanoparticles preceded the understanding of nanoscale phenomena. Systematic studies of nanoparticles began to appear as early as the seventeenth century. Antonio Neri, a Florentine glass maker and priest, describes the synthesis of colloidal gold in his 1612 treatise *L'Arte Vetraria*. John Kunckel, revised and translated Neri's work into german in 1689. Kunckel is often credited with the discovery that glass can be colored red by addition of gold.

Despite the early advances, studies of nanoscale particles did not gather momentum in later years. Thus, for most part of the 20th century, colloid science was the domain of a few specialized groups and did not receive sufficient importance. As early as 1857, Michael Faraday [4] carried out ground-breaking work on colloidal metals. He called them divided metals. Faraday established the very basis for the area, noting that colloidal metal sols were thermodynamically unstable, and that the individual particles must be stabilized kinetically against aggregation. Note that sols are dispersions of solids in liquids. Once the particles in a sol coagulate, the process cannot be reversed. Remarkably, Faraday also identified the essence of the nature of colloidal, nanoscale particles of metals. In the case of gold, he stated "gold is reduced in exceedingly fine particles which becoming diffused, produce a beautiful fluid ... the various preparations of gold whether ruby, green, violet, or blue ... consist of that substance in a metallic divided state." Einstein [5] related the Brownian motion executed by the nanoparticles to their diffusion coefficient. Mie and Gans [6–8] proposed a theoretical basis for the optical properties of the nanoscale particles, which continues to be used widely to this day. Frölich and Kubo proposed

theories that predicted that the electronic structure of colloidal metals would differ from bulk.

The neglect of colloid science prompted Ostwald [9] to title his 1915 book on colloids as "The world of neglected dimensions." This period also witnessed advances in methods to make colloidal gold. Bredig [10] prepared Au sols by striking an arc between Au electrodes immersed in dilute alkali. Donau [11] suggested that passing CO through a solution of chloroauric acid provided a gold sol. Zsigmondy [12] discovered the seeding method and was familiar with the use of formaldehyde in mild alkali to produce Au sols from salts. The 1925 award of the Nobel prize to Zsigmondy partly for his work on gold colloids did not seem to have enthused the scientific community to pursue this area of research. In the last few years, however, there has been a great upsurge in the use of colloid chemical methods to generate nanoparticles of various materials. This is because of the excitement caused by the science of nanomaterials initiated by the now famous lecture of Feynman [13].

Explosion of research in nanocrystals has been so dramatic that very few of the modern practitioners seem to be aware of the glorious past of colloid science. The progress has been facilitated in part by the advances in instrumentation that have helped in fully characterizing nanomaterials. Today, it is possible to prepare and study nanocrystals of metals, semiconductors and other substances by various means. Advances in both experimental and theoretical methods have led to an understanding of the properties of nanocrystals.

1.2 Properties of Nanocrystals

Nanocrystals of materials are generally obtainable as sols. Sols containing nanocrystals behave like the classical colloids. For example, the stability of a dispersion depends on the ionic strength of the medium. Nanocrystalline sols possess exceptional optical clarity. A key factor that lends stability to nanocrystal sols is the presence of a ligand shell, a layer of molecular species adsorbed on the surface of the particles. Without the ligand shell, the particles tend to aggregate to form bulk species that flocculate or settle down in the medium. Depending on the dispersion medium, the ligands lend stability to particles in two different ways. Thus, in an aqueous medium, coulomb interactions between charged ligand species provide a repulsive force to counter the attractive van der Waals force between the tiny grains, by forming an electrical double layer. In an organic medium, the loss of conformational freedom of the ligands and the apparent increase in solute concentration provide the necessary repulsive force. We illustrate this schematically in Fig. 1.2. Nanocrystals dispersed in liquids are either charge-stabilized or sterically stabilized.

Nanoparticles devoid of ligands are generally studied in vacuum. Such particles deposited on a substrate are readily examined by photoelectron spectroscopy and other techniques. Beams of uniformly sized clusters traversing

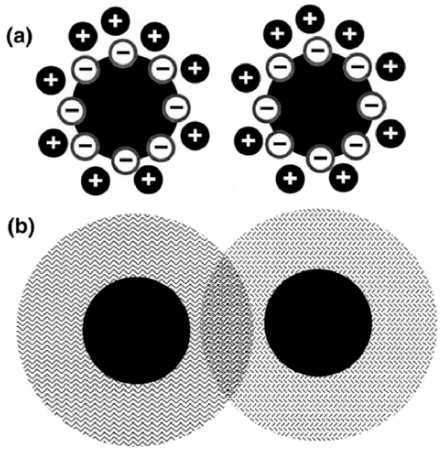

Fig. 1.2. Schematic illustration of the factors lending stability to a colloidal dispersion: (**a**) an electric double layer and (**b**) loss of conformational freedom of chain-like ligands

a vacuum chamber (cluster beams) with some fixed velocity provide opportunities for studies of the intrinsic physical properties of nanoparticulate matter.

1.2.1 Geometric Structure

The dimensions of nanocrystals are so close to atomic dimensions that an unusually high fraction of the total atoms would be present on their surfaces. For example, a particle consisting of 13 atoms, would have 12 atoms on the surface, regardless of the packing scheme followed. Such a particle has a surface more populated than the bulk. It is possible to estimate the fraction of atoms on the surface of the particle (P_s, percentage) using the simple relation,

$$P_\mathrm{s} = 4N^{-1/3} \times 100, \tag{1.1}$$

where N is the total number of atoms in the particle [14]. The variation of the surface fraction of atoms with the number of atoms is shown in Fig. 1.3. We see that the fraction of surface atoms becomes less than 1% only when the total number of atoms is of the order of 10^7, which for a typical metal would correspond to a particle diameter of 150 nm.

Nanoparticles are generally assumed to be spherical. However, an interesting interplay exists between the morphology and the packing arrangement, specially in small nanocrystals. If one were to assume that the nanocrystals strictly follow the bulk crystalline order, the most stable structure is arrived at by simply constraining the number of surface atoms. It is reasonable to assume that the overall polyhedral shape has some of the symmetry elements of the constituent lattice. Polyhedra such as the tetrahedron, the octahedron,

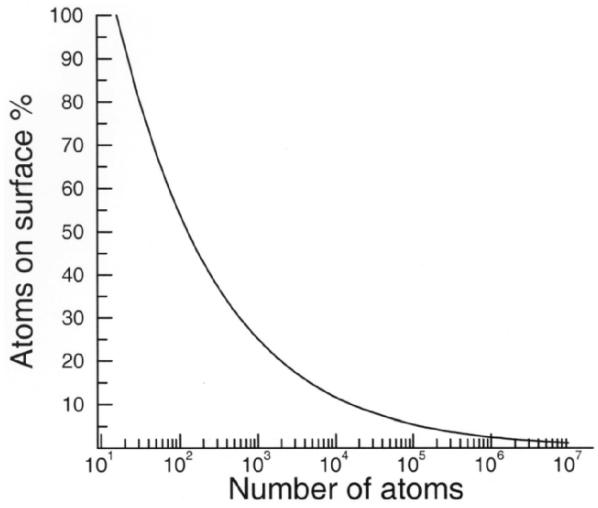

Fig. 1.3. Plot of the number of atoms vs. the percentage of atoms located on the surface of a particle. The calculation of the percentage of atoms is made on the basis of (1.1) and is valid for metal particles

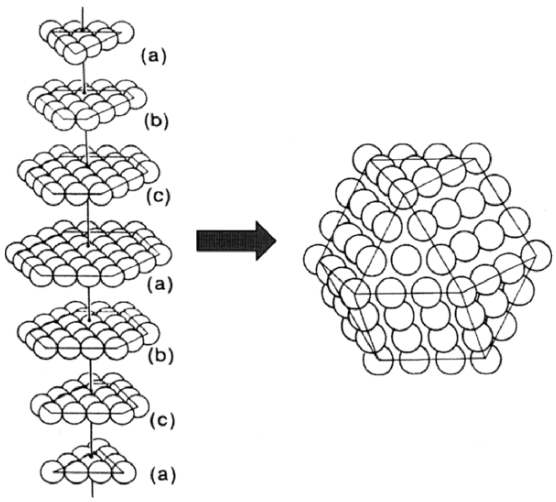

Fig. 1.4. Schematic illustration of how a cuboctahedral 147 atom-cluster, composed of seven close-packed layers can be made out of a stacking sequence reminiscent of a fcc lattice (reproduced with permission from [16])

and the cuboctahedron can be constructed following the packing scheme of a fcc lattice [15, 16]. Figure 1.4 shows how a cuboctahedral cluster of 146 constituent atoms follows from a fcc type *abcabc* layer stacking. In contrast to the above, small clusters frequently adopt *non-close packed* icosahedral

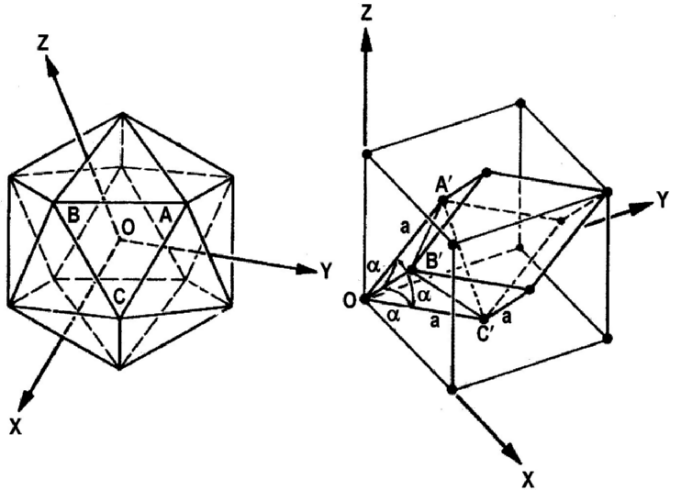

Fig. 1.5. The regular icosahedron is made up of twenty irregular tetrahedra like OABX. The rhombhohedral cell in a fcc lattice (OA′B′C′) has $\alpha = 60°$. When α is distorted to 63.43°, OA′B′C′ and OABC become similar. Small nanocrystals distort in a similar manner from regular fcc lattice to adopt the icosahedral shape

or dodecahedral shapes. The clusters adopting such schemes suffer a loss in packing efficiency. The icosahedron has a fivefold symmetry, inconsistent with the packing requirements of a regular crystalline lattice with long-range order. While employing close packing schemes, a stacking fault becomes necessary to arrive at an icosahedral arrangement. Such a scheme is outlined in Fig. 1.5.

The icosahedron which has twenty triangular faces and twelve vertices consists of a fcc-like close packing. Each of the twenty triangular faces of an icosahedron can be considered as a base of a tetrahedron, whose apex is at the inversion center (see Fig. 1.5a). A tetrahedron OA′B′C′ in Fig. 1.5b joining three face-centered atoms and an atom at the base of a fcc unit cell has the angle, $\alpha = 60°$. These angles can be distorted to 63.43°, to obtain the tetrahedron (OABC) that forms the building block of an icosahedron. Such a distortion results in the lowering of the packing fraction from 0.74080 to 0.68818. Several theoretical investigations have sought to explain the unusual stability of icosahedral clusters [17–19]. Allpress and Sanders [20, 21], based on potential energy calculations, showed that the binding energy per atom is lower than that in a corresponding octahedron containing the same number of atoms. Molecular dynamics simulations have shown that Al clusters with nuclearities upto 147 atoms exhibit distorted icosahedral structures while Al_{147} has a cuboctahedral shape [22]. More rigourous theories (ab initio, density functional) broadly support this contention. A decahedral shape can be thought of as being made up of four edge-sharing tetrahedra, followed by some relaxation and the consequent loss of packing fraction. Ino [23, 24]

has suggested the use of the term "multiply twinned particle" to denote a decahedral particle, and such particles obtained by the twining of tetrahedra.

The properties of nanocrystals are also influenced by the formation of geometric shells which occur at definite nuclearities [25, 26]. Such nuclearities, called magic nuclearities endow a special stability to nanocrystals as can be demonstrated on the basis of purely geometric arguments. A new shell of a particle emerges when the coordination sphere of an inner central atom or shell (forming the previous shell) is completely satisfied. The number of atoms or spheres required to complete successive coordination shells is a problem that mathematicians, starting with Kepler, have grappled with for a long time [27, 28]. The "kissing" problem, as it is known in the mathematical world, was the subject of a famous argument between Newton and Gregory at Cambridge. In retrospect, Newton, who held that 12 atoms are required to complete the second shell was indeed correct. An idea of the mathematical effort involved can be gauged from the fact that the proof of Newton's argument was provided only in 2002. It is quite apparent that the ultimate shape of the emerging crystallite should play a role in determining the number of atoms that go into forming complete shells. The magic nuclearities would then yield information on the morphology of the cluster. By a strange coincidence, the number of atoms required to form complete shells in the two most common shapes (icosahedron and cuboctahderon) is the same.

The number of atoms, N, required to form a cluster with L geometric shells is given by

$$N = \frac{(10L^3 + 15L^2 + 11L + 3)}{3}. \tag{1.2}$$

This represents the solution for the "kissing" problem in three dimensions and is valid for icosahedral and cuboctahedral morphologies. For other shapes, the reader may refer to a paper from the group of Martin [29]. Particles possessing the above number of atoms are said to be in a closed-shell configuration. The number of atoms required to fill up coordination shell completely, n_L of a particular shell, is given by

$$n_L = (10n_{L-1}^2 + 2). \tag{1.3}$$

where n_0=1. Thus, 12 atoms are required to complete the first shell, 42 to complete the second shell etc. A schematic illustration of the observed magic nuclearity clusters is provided in Fig. 1.6. The notion of the closed-shell configuration can be extended to larger dimensions as well. Closed-shell configurations lend stability to giant clusters made of clusters and even to a cluster of giant clusters.

Determination of the structures of nanocrystals should ideally follow from X-ray diffraction, but small particles do not diffract well owing to their limited size. The peaks in the diffraction pattern are less intense and are broad. Structural studies are therefore based on high resolution transmission electron microscopy (HRTEM), extended X-ray absorbtion fine structure (EXAFS),

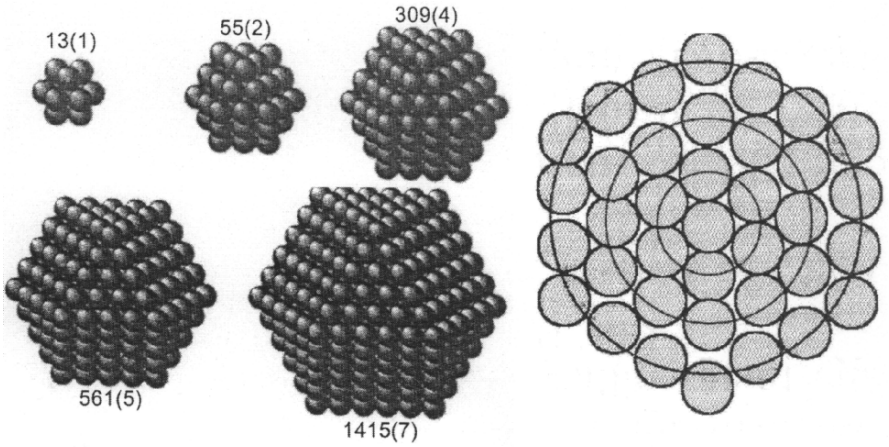

Fig. 1.6. Nanocrystals in closed-shell configurations with magic number of atoms. The numbers beside correspond to the nuclearity (N) and the number of shells (L). The figure on the left is a cross-sectional view showing five coordination shells in a 561 atom cluster

scanning tunneling microscopy (STM) and atomic force microscopy (AFM). X-ray diffraction patterns provide estimates of the diameters (D) of nanocrystals from the width of the diffraction profiles, by the use of the Scherrer formula [30]

$$D = \frac{0.9\lambda}{\beta\cos\theta}. \tag{1.4}$$

Here, β is the full-width at half-maximum of the broadened X-ray peak corrected for the instrumental width,

$$\beta = \beta^2_{\text{observed}} - \beta^2_{\text{instrumental}}. \tag{1.5}$$

Estimates based on the Scherrer relation are used routinely. It is desirable to carry out a Reitveld analysis of the broad profiles of nanoparticles to obtain estimates of D.

HRTEM with its ability to image atomic distributions in real space, is a popular and powerful method. The icosahedral structure of nanocrystals is directly observed by HRTEM and evidence for twinning (required to transform a crystalline arrangement to an icosahedron) is also obtained by this means (see Fig. 1.7) [15, 31]. The images are often compared with the simulated ones [32, 33]. High resolution imaging provides compelling evidence for the presence of multiply twinned crystallites specially in the case of Au and Ag nanoparticles [34]. Characterization by electron microscopy also has certain problems. For example, the ligands are stripped from the clusters under the electron beam; the beam could also induce phase transitions and other dynamic events like quasi-melting and lattice reconstruction [35]. The fact

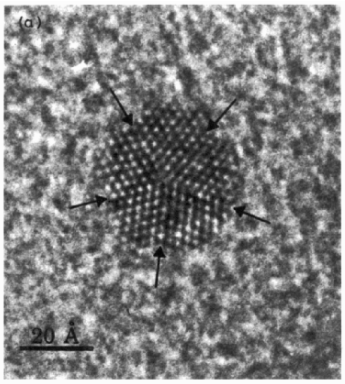

Fig. 1.7. A high resolution TEM image showing the icosahedral shape and the five fold symmetry axis of a Ag nanoparticle (reproduced with permission from [31])

that ligands desorb from clusters has made it impossible to follow the influence of the ligand shell on cluster packing.

STM, with its ability to resolve atoms, provides exciting opportunities to study the size and morphology of individual nanoparticles. In the case of ligated nanocrystals, the diameters obtained by STM include the thickness of the ligand shell [36]. Ultra high vacuum STM facilitates in situ studies of clusters deposited on a substrate. Furthermore, it is possible to manipulate individual nanoscale particles using STM. However, it is not possible to probe the internal structure of a nanocrystal, especially if it is covered with a ligand shell. AFM supplements STM and provides softer ways of imaging nanocrystals. EXAFS has advantages over the other techniques in providing an ensemble average, and is complimentary to HRTEM [37].

1.2.2 Magnetic Properties of Nanocrystals

Isolated atoms of most elements possess magnetic moments that can be arrived at on the basis of Hund's rules. In the bulk, however, only a few solids are magnetic. Nanoscale particles provide opportunities to study the evolution of magnetic properties from the atomic scale to the bulk. Even before the explosion of interest in nanoscience, magnetic properties of the so-called fine particles had been examined. In fact, size effects were perhaps first noticed in magnetic measurements on particles with diameters in the 10–100 nm range [38].

In order to understand size-dependent magnetic properties, it is instructive to follow the changes in a magnetic substance as the particle size is decreased from a few microns to a few nanometers. In a ferromagnetic substance, the T_c decreases with decrease in size. This is true of all transition temperatures associated with long-range order. For example, ferroelectric transition temperatures also decrease with particle size. With the decrease in the diameter,

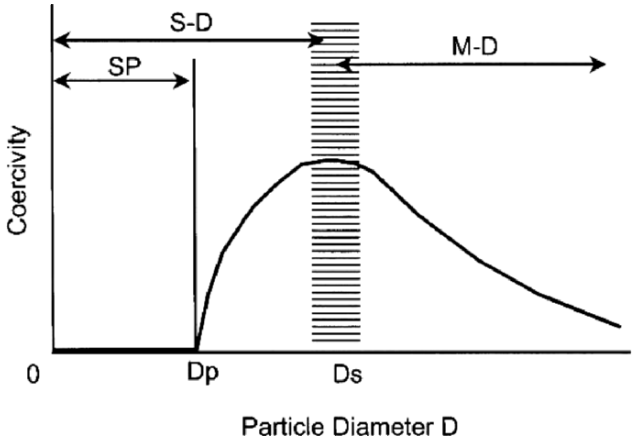

Fig. 1.8. Schematic illustration of the change in the coercivity of a ferromagnetic particle with the diameter. SP denotes the superparamagnetic regime, S-D the single-domain regime and M-D the multi-domain regime

the coercivity (H_c), increases initially till a particular diameter, D_s, and thereafter decreases as shown in Fig. 1.8. The critical diameter, D_s, marks a region wherein the particle changes from being a multi-domain particle to a single-domain particle. The value of D_s is normally a few tens of nanometers. The single-domain nature of the nanoparticle is its single most attractive magnetic property. Below D_s, H_c tends to decrease due to thermal effects and follows a relation of the form:

$$H_c = g - \frac{h}{D^{3/2}}, \tag{1.6}$$

where g and h are constants [39]. Below the critical diameter D_p, coercivity becomes zero as the thermal energy would be sufficient to randomize the magnetic moments in the particle. Nanocrystals below the diameter D_p ($\sim$10 nm), exhibit such a behavior and are said to be superparamagnetic. Superparamagnetic particles do not possess long-range magnetic order, but show characteristic magnetic properties at low temperatures [40]. Particles delineated on the basis of the above critical regimes, follow different paths to the final magnetized state and the magnetization reversal mechanism. These paths and mechanisms are rather complicated [39].

Size-dependent changes in magnetic anisotropy are another aspect of interest. A magnetic material exhibits strong and often complex anisotropic behavior when subjected to magnetization. The magnetic anisotropic energy (E), defined as the energy difference involved in changing the magnetization direction from a low-energy direction or easy axis to a high energy direction or hard axis, is an important technological parameter. Materials with high E and low E find numerous applications. The simplest form of anisotropy is the uniaxial anisotropy, where E is only dependent on the angle that the magnetic

field vector makes with the easy axis of the sample. Square hysteresis loops are obtained when the direction of magnetization is parallel to the easy axis and a straight line response is obtained when the field direction is perpendicular to the easy axis direction [41, 42]. Materials are also known to exhibit hexagonal and cubic anisotropy. The nature of magnetic anisotropy can be arrived at by studying hysteresis loops obtained along various directions. E exhibits dramatic changes with the change in size and shape. Nanoparticles generally possess higher E, but may also show a change in the basic nature of anisotropy.

Superparamagnetic behavior is caused by thermal flipping of the anisotropic barrier to magnetization reversal. Below a certain temperature, called the blocking temperature, temperature-induced flipping or relaxation can be arrested and the nanocrystals acquire a finite coercivity. In Fig. 1.9, magnetic measurements indicating size-dependent changes in the blocking temperature of $CoFe_2O_4$ nanoparticles are shown. The superparamagnetic behavior was first modeled by Neel in the 1950s [43]. In the case of nanoparticles with uniaxial anisotropy, Neel's theory suggests that the temperature induced relaxation varies exponentially with temperature and scales with the sample volume. Besides the loss of coercivity, another characteristic feature

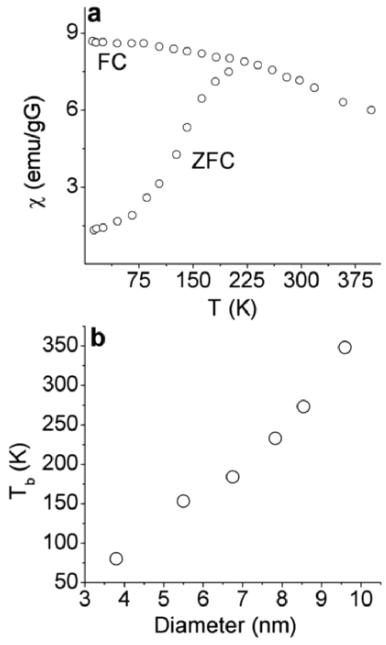

Fig. 1.9. (**a**) Magnetic susceptibility vs. temperature for $CoFe_2O_4$ nanoparticles under field cooled and zero-field cooled conditions. The applied field is 2,000 G. (**b**) shows the variation of blocking temperature (T_b) with diameter of nanoparticles (plot produced with data from [40])

of superparamagnetic behavior is the scaling of magnetization with temperature. A plot of the magnetization (M) and the ratio of the magnetic field and the temperature (H/T) produces a universal curve for all temperatures above T_b. Experimentally, superparamagnetism may be probed by techniques such as neutron scattering, Mössbauer spectroscopy and magnetization measurements. Since superparamagnetic behavior is related to the relaxation rate, it is sensitive to the characteristic time scale of measurement. In the experimental techniques indicated above, the time scales of measurements vary over a wide range (10^{-14}–10^{-12} for neutron scattering to around 10 s for magnetization measurement) and different measurements, therefore, yield different blocking temperatures. Though the scaling with volume suggested by the Neel theory is largely followed in the uniaxial cases, the actual blocking behavior of magnetic nanocrystals, especially those of the oxides are quite complicated. Effects due to the ligand shell and lattice defects are generally considered to be responsible for the observed deviations.

Many metal oxide nanoparticles are known to show evidence for the presence of ferromagnetic interactions at low temperatures. This is specially true of nanoparticles of antiferromagnetic oxides such as MnO, CoO, and NiO [44,45]. What one normally observes is a divergence in the zero-field cooled and field cooled magnetization data at low temperatures. The materials show magnetic hysteresis below a blocking temperature typical of superparamagnetic materials. The blocking temperature generally increases with the particle size. In Fig. 1.10, we show the magnetization behavior of NiO particles of 3 and 7 nm diameters [45].

While reasonable progress has been made in understanding the magnetic properties of isolated particles, ensembles of particles represent a relatively poorly researched area [46, 47]. A typical ensemble consists of particles with distributions in size, shape and easy anisotropy direction. Further, interparticle interactions play a role in determining the magnetic response of the ensemble. Theoretical investigations predict interesting phenomena in such assemblies, including changes in the mechanism of magnetization, depending on interparticle interactions. Experimentally, controlled interactions are brought about by varying parameters such as the volumetric packing density. Experiments have been carried out on ensembles of nanoparticles obtained in various ways such as freezing a sol containing a known fraction of magnetic nanoparticles or dilution in a polymer matrix [41, 46–48]. Seminal advances have been made in obtaining such ensembles by self-assembly based techniques. Self-assembled nanocrystalline ensembles posses several advantages over those obtained by other means.

1.2.3 Electronic Properties

Bulk metals possess a partially filled electronic band and their ability to conduct electrons is due to the availability of a continuum of energy levels above E_F, the fermi level. These levels can easily be populated by applying an